Supporting Information

High efficiency InAs/GaAs quantum dot solar cell due to inter-dot n-doping

K. A. Sablon and J. W. Little
U.S.Army Research Laboratory, Adelphi, MD 20783
V. Mitin, A. Sergeev, N. Vagidov
University at Buffalo, Buffalo, NY 14260
K. Reinhardt
Air Force Office for Scientific Research

(i) Photoluminescence of n- and p-doped QD structures.

The room temperature photoluminescence (PL) in QDoSCs has been measured under the short circuit conditions to match to the short circuit current measurements. To stimulate the PL we used the 532 nm line from a frequency-doubled neodymium doped yttrium aluminum garnet (Nd:YAG) laser with the 20 μm diameter of the laser spot on a sample. The PL signals from the samples were measured by an InGaAs detector array. The PL spectra were obtained under excitation intensities of 0.3, 0.5, 1, and 4 W/cm^2. PL data for low intensities are presented in the main text. Figure 1 shows the spectral dependence of the PL on the doping level in n-doped samples under intensity of 0.5 W/cm^2.

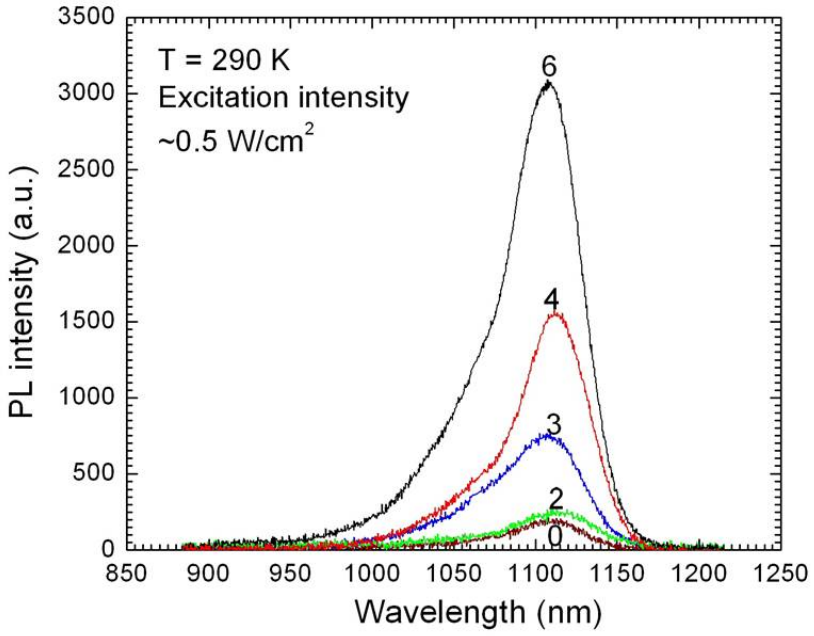

Fig. 1. Spectral dependence of PL in QD sample with 0, 3, 4, and 6 electrons per dot under 0.5 W/cm^2 intensity.

Figures 2 and 3 present the spectral dependences of the PL at various doping levels under higher intensities, 1 and 4 W/cm^2.

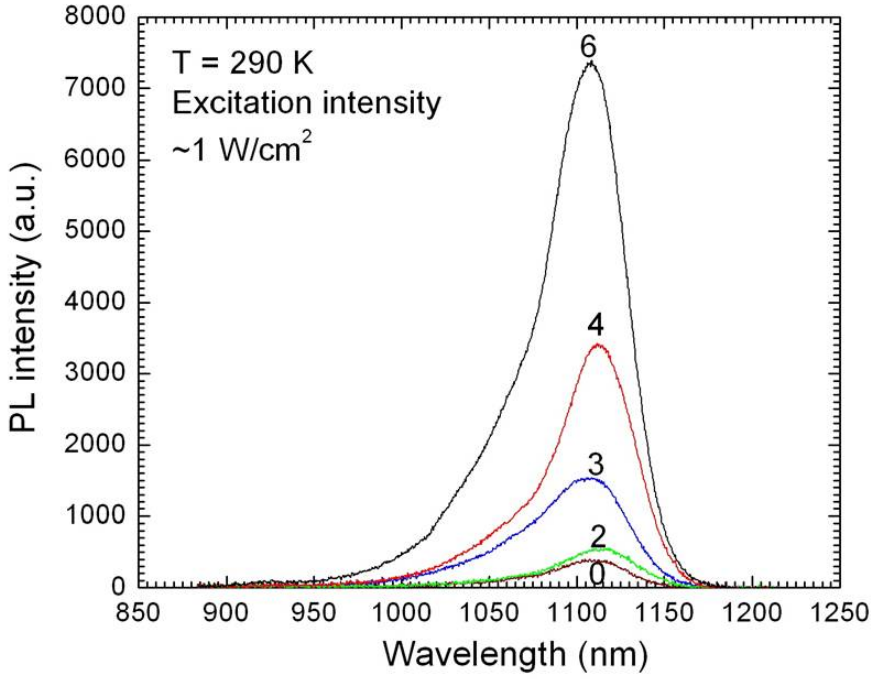

Fig. 2. Spectral dependence of PL in QD sample with 0, 3, 4, and 6 electrons per dot under 1 W/cm^2 intensity.

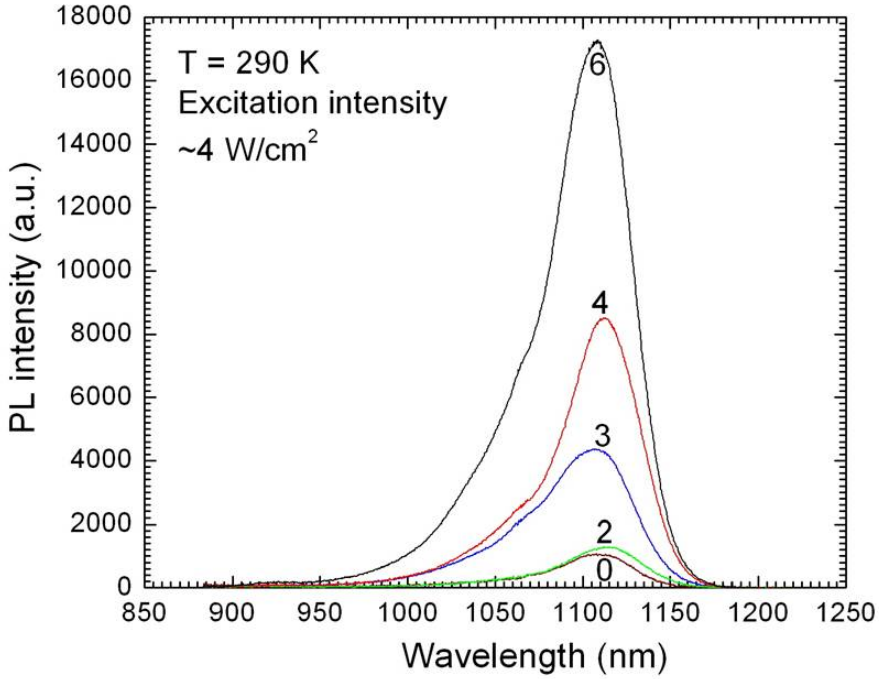

Fig. 3. Spectral dependence of PL in QD sample with 0, 3, 4, and 6 electrons per dot under 4 W/cm^2 intensity.

As seen from Figs. 1-3, the PL substantially increases with doping.

In Figs. 4 and 5 we compare the photoluminescence from p- and n-doped samples under 1 and 4 W/cm^2 intensities.

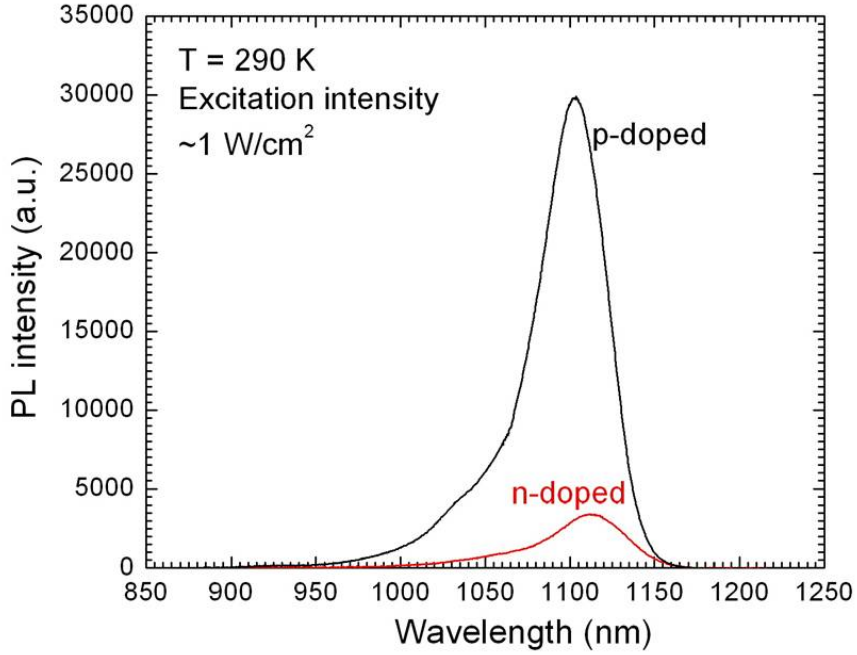

Fig. 4. Comparison of PL spectral dependences of n- and p-doped samples with 4 carriers per dot under 1 W/cm^2 intensity.

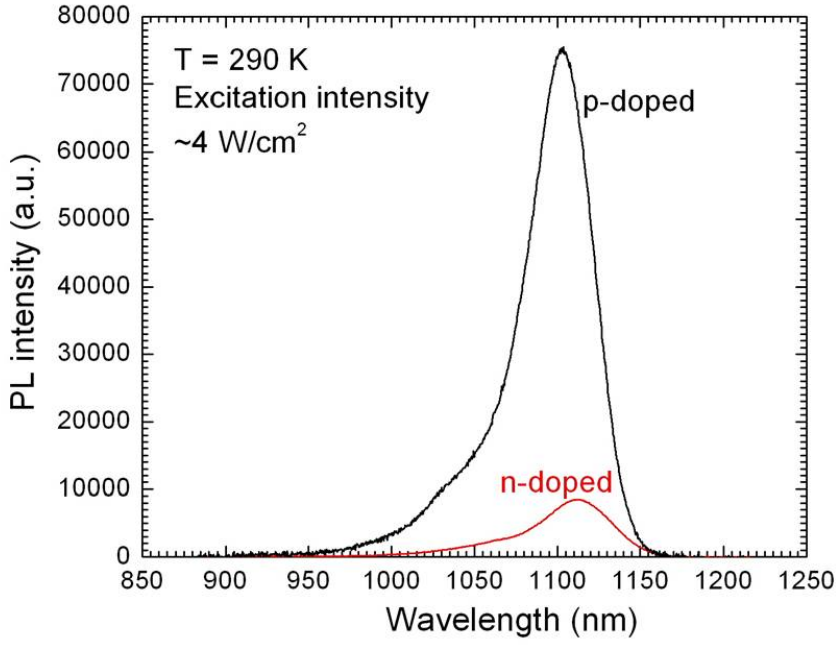

Fig. 5. Comparison of PL spectral dependences of n- and p-doped samples with 4 carriers per dot under 4 W/cm^2 intensity.

It is important to highlight that Figs. 4 and 5 present the PL of p- and n-doped samples with the same level of doping, which corresponds to four carriers per dot. As seen, the PL intensity from the p-doped sample significantly exceeds that of the n-doped sample. The ratio of PL from p- and n-doped samples just slightly depends on the radiation intensity. These data directly evidence that the capture/relaxation rate for electrons is substantially higher than that for holes. It is also clearly seen that the PL maximum of the p-doped sample is shifted toward the shorter wavelength regime with respect to the corresponding maximum for the n-doped sample. According Ref. 1, this many-body effect is also direct evidence of the accumulation of the corresponding carriers – electrons in n-doped samples and holes in p-doped samples – in quantum dots. For the photovoltaic applications, it is necessary to minimize the recombination losses, i.e. to increase the photocarrier lifetime. Therefore, n-doping is more favorable for QDoSC operation.

(ii) Carrier capture processes

Following to our works,[2,3] we consider a quantum-dot structure with the potential barriers around dots. In what follows the detailed form of the barriers is not critical. The only important assumption we accept here is that the probability of tunnelling processes is small compared with the capture probability via thermo-excitation above the potential barrier. For example, for dots with a ~ 10 nm the potential that satisfies the above condition can be created by the homogeneous doping of the interdot space. Without tunneling processes, the photoelectron capture rate,

$$\tau_{capt}^{-1} = N_d \sigma \tilde{v} , \tag{1}$$

is given by the equation for the trapping cross-section,[2,3]

$$\sigma = \pi \alpha a^2 \exp\left(-\frac{eV_m}{kT}\right)\left(1+\frac{3}{4}\frac{\alpha a}{\ell}F(V)\right)^{-1} , \tag{2}$$

$$F = a \exp\left(-\frac{eV_m}{kT}\right)\int_a^b \frac{dr}{r^2}\exp\left(\frac{eV(r)}{kT}\right) , \tag{3}$$

where $\tilde{v}$ is the electron thermal velocity, N_d is the concentration of quantum dots, a is the radius of the dot, b is the interdot distance, ℓ is the electron mean free path with respect to elastic electron scattering, α is the probability for an electron at $r \le a$ to be captured by the quantum dot, and V_m is the maximum value of the potential barrier, *i.e.* $V_m = V(a)$.

We would like to emphasize that Eqs. (2) and (3) are valid for any relation between ℓ, a, and αa as well as for wide variety of potential profiles. As a simple example, let us consider the flat potential profile $V = 0$. In this case,

$$\sigma = \pi\alpha a^2\left[1+\frac{3}{4}\frac{\alpha a}{\ell}\right]^{-1}. \qquad (4)$$

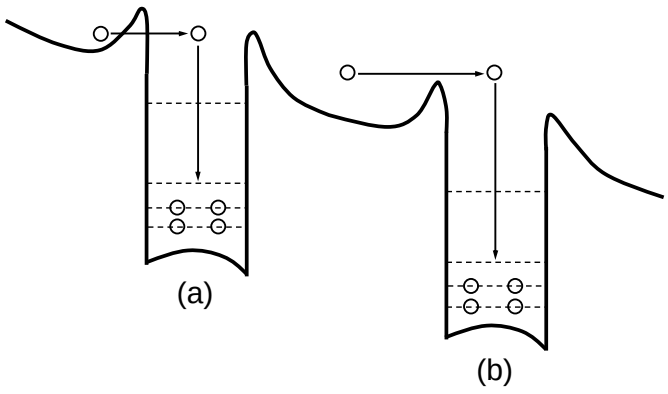

Fig. 6. Photoelectron capture due to electron tunneling (a) and thermo-excitation (b).

As it is presented in Fig. A, the carrier capture can be realized via electron tunneling (a) or via thermo-excitation above the potential barriers (b). Relative probability of tunneling and thermo-excitation capture processes can be evaluated taking into account the position of the turning point for electron tunneling. Assuming that the barrier potential near the dot is close to the Coulomb potential, the position of the turning point, R_t, averaged over the thermal electron distribution is given by:

$$R_t = a_B\left(\frac{Ry}{kT}\right)^{2/3}\left(Zm^*\right)^{1/3}, \qquad (5)$$

where a_B is the Bohr radius, Ry is the Rydberg constant, Z is the charge of the dot, and m^* is the electron effective mass. In particular, for GaAs at room temperatures, R_t is about 4 nm. If the dot radius is larger than R_t the thermo-excitation will dominate over tunneling. In the rest of the paper we will consider exactly this case.

Describing the thermo-excitation processes, we will accept that the inelastic intradot relaxation processes are described by the relaxation time τ'_ε. In this case, the coefficient α can be evaluated as $\alpha \approx a/\ell'_\varepsilon$, where $\ell'_\varepsilon = \tilde{v}'\tau'_\varepsilon$ and $\tilde{v}'$ is the electron thermal velocity in the dot. Then, if $a^2 << \ell\ell'_\varepsilon$, we obtain the capture rate:

$$\frac{1}{\tau_{capt}} = \pi N_d a^3 \frac{\tilde{\nu}}{\tilde{\nu}'} \frac{1}{\tau'_\varepsilon} \quad . \tag{6}$$

In the opposite case, $a^2 >> \ell\ell'_\varepsilon$, the capture rate is independent of the coefficient α and is

$$\frac{1}{\tau_{capt}} = 4\pi N_d D\, a \ , \tag{7}$$

where $D = \tilde{\nu}\ell/3$ is the diffusion coefficient. Note, that the second term in the square brackets in Eq. (2) describes the reduction of the carrier concentration near the dot due to the capture processes. As we discussed, this effect becomes important in the electron capture, if $\ell < \alpha\, a$, and which results in Eq. (7). In the opposite case, the electron concentration is practically homogeneous in space and carrier capture is determined by Eq. (6).

Returning to the capture processes in the presence of potential barriers, we should note that the second term in the brackets in Eq. (2) also describes the reduction of the carrier concentration near the dot. Due to the repulsive potential barriers this effect is increased by a factor of *F* (*V*) given by Eq. (3). The *F(V)* may be associated with the Sommerfeld factor, which shows the reduction of carrier density (electron wave function) near the trap. If local reduction of carrier density is negligible, then the capture rate is:

$$\frac{1}{\tau_{capt}(V)} = \frac{1}{\tau_{capt}(0)} \exp\left(-\frac{eV_m}{kT}\right), \tag{8}$$

where the exponential factor describes the effect of potential barriers on capture processes.
Summarizing, we should note that, the carrier capture regime changes when the characteristic dot size becomes comparable with the electron mean free path (see Eqs. 6 and 7). The carriers trapped in the dot create potential barriers, which suppress the capture of the like charges. This effect has strong exponential dependence on the trapped charge (Eq.8).

(iii) Conversion efficiency and the filling factor

In Fig. 7 we present the photovoltaic conversion efficiency as a function of the bias voltage for the GaAs reference solar cell, undoped, p- and n-doped QDoSCs. These dependences have been directly obtained from the corresponding *I-V* characteristics presented in Fig. 3 of the paper.

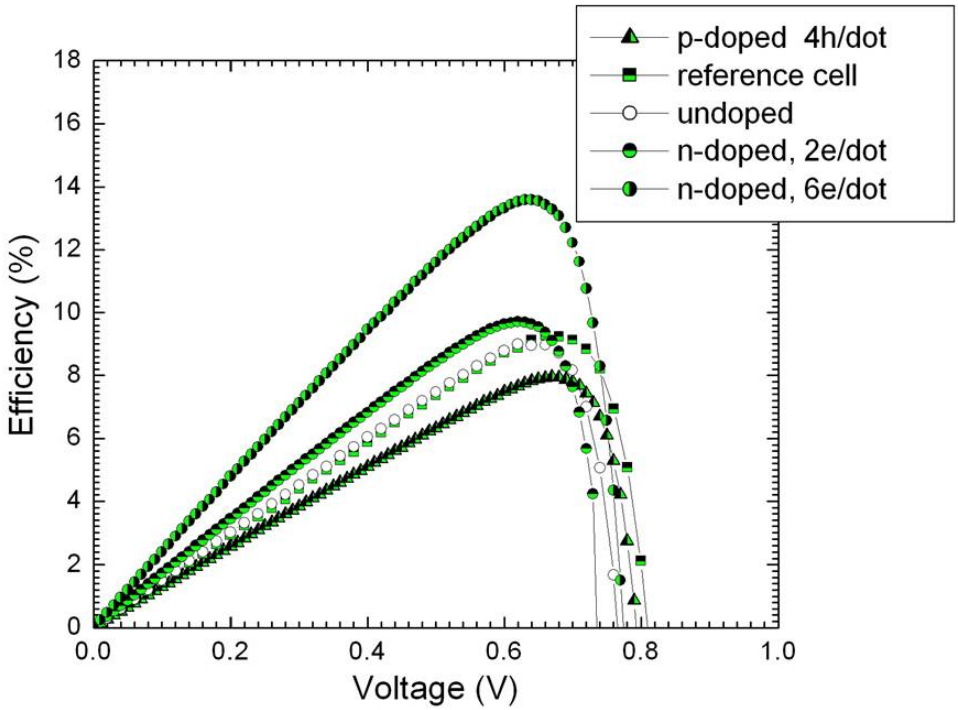

Fig. 7. Conversion efficiency vs bias voltage for GaAs reference cell, undoped, p-doped (4 holes per dot), and n-doped QDoSCs (2 and 6 electrons per dot).

The corresponding filling factors have been found to be 77%, 75%, and 72% for undoped and n-doped QDoSCs with 2 and 6 electrons per dot, correspondingly.

References

[1] D. V. Regelman, E. Dekel, D. Gershoni, E. Ehrenfreund, A. J. Williamson, J. Shumway, and A. Zunger, W. V. Schoenfeld, and P. M. Petroff, *Phys. Rev. B* **2001**, 64, 165301.

[2] A. Sergeev, V. Mitin, and M. Stroscio, *Physica B* **2002**, 316-317, 369.

[3] V. Mitin, A. Sergeev, L.-H. Chien, and N. Vagidov, *Proc. SPIE* **2008**, 7095, 70950K.